

Time evolution of positron affinity trapping at embedded nanoparticles by age-momentum correlation

K. Inoue,^{1,2} Y. Nagai,¹ Z. Tang,^{3,4} T. Toyama,¹ Y. Hosoda,¹ A. Tsuto,¹ and M. Hasegawa^{3,5}

¹*The Oarai Center, Institute for Materials Research, Tohoku University, Oarai, Ibaraki 311-1313, Japan*

²*Department of Materials Science and Engineering, Graduate School of Engineering, Kyoto University, Yoshida Honmachi, Sakyo-ku, Kyoto 606-8501, Japan*

³*Institute for Materials Research, Tohoku University, Sendai, Miyagi 980-8577, Japan*

⁴*Key Laboratory of Polar Materials and Devices (Ministry of Education of China), East China Normal University, Shanghai 200241, People's Republic of China*

⁵*Cyclotron and Radioisotope Center, Tohoku University, Sendai, Miyagi 980-8578, Japan*

(Received 14 January 2011; published 31 March 2011)

A positron annihilation age-momentum correlation (AMOC) technique using a digital oscilloscope with high time resolution enabled us to directly estimate positron trapping rate to nano- and subnanoparticles embedded in materials by observing the annihilation time evolution of the momentum distribution of affinity-trapped positron-electron pairs. As a representative case we successfully apply the present technique to (sub)nano Cu particles embedded in an Fe-Cu dilute alloy after thermal aging. This enhances the ability of the positron annihilation method as a quantitative tool to detect ultrafine embedded particles which are difficult to observe by other techniques. We also show that the AMOC measurements give chemical information on the embedded particles through the positron trapping kinetic behavior.

DOI: [10.1103/PhysRevB.83.115459](https://doi.org/10.1103/PhysRevB.83.115459)

PACS number(s): 68.65.-k, 73.21.La, 73.22.-f, 78.70.Bj

I. INTRODUCTION

(Sub)nano embedded particles (SNEPs) in materials are very important because of their many industrial prospective applications, such as ultrafine precipitates in electronic and structural materials. Information on the SNEPs, such as size, number density, chemical composition, and electronic structure, is indispensable for understanding physical and mechanical properties of the materials. Various experimental tools, such as transmission electron microscope,¹ the three-dimensional atom probe (3D-AP),^{2,3} and small-angle neutron scattering,⁴ have been adopted for this purpose. However, these techniques still have difficulties related to the limited minimum size of detectable SNEPs. Therefore, a method which can overcome these difficulties is strongly desired. Here we propose a method using positron annihilation.

It is well known that a positron, an antiparticle of an electron, is sensitive to vacancy-type defects.⁵ However, in the year 2000, we found that the positron is a site-selective probe for such SNEPs;⁶ the positron can be confined in SNEPs with higher positron affinities than that of the host,^{7,8} even if the SNEPs are free from open-volume defects.^{6,8,9} We call this affinity-induced confinement a positron quantum-dot-like state.⁶ The thermalized positron diffuses about a few hundred nanometers before annihilation⁷ and can be trapped at one of the SNEPs in the diffusing volume, which makes positrons a very sensitive probe of the SNEPs. In addition, the minimum detectable size, depending on the difference of the positron affinity between the SNEP and the host, is typically less than a few nanometers in diameter (for example, even only about ten atoms in the case of Cu clusters in an Fe host^{6,10,11}), which shows the excellent sensitivity for SNEPs at the very initial stages of their formation which are difficult to observe by the conventional techniques stated above. Furthermore the confined positrons exclusively annihilate with the electrons

of the SNEP and thus bring site-selective information on the chemical composition and electronic structures of the SNEP.

We have been developing various kinds of estimation methods using the unique characteristic of the positron quantum-dot-like state in order to reveal the size, the chemical composition, and the electronic structure. The chemical composition is determined by measuring the momentum distribution of core electrons, characteristic of each chemical element, using the coincidence Doppler broadening (CDB) method.^{6,10} The electronic structures of the SNEP were elucidated by Fermi surface observation using the two-dimensional angular correlation of annihilation radiation (2D-ACAR) method.^{11,12} The sizes of the SNEPs can be determined by the momentum smearing around the Fermi momentum measured by 2D-ACAR.^{13,14} The highlight of this work is that we can estimate the number density of the SNEPs by observing the annihilation time evolution of the momentum distribution of the affinity-trapped positron-electron pairs.

In the case of vacancy-type defects, the positron lifetime is usually employed to estimate their sizes and number densities. The positron annihilation rate in the defects is much lower than that in the bulk since the electron density in the defect is lower than that in the bulk. Thus, the open-volume sizes of the defects can be determined by the positron lifetime at the defects and the positron trapping rate to the defects, proportional to the defect number density, can be determined by using a simple positron trapping model.⁵ Unfortunately, the conventional positron lifetime method is usually not applicable to the SNEPs with positron affinity that are free from open-volume defects, because the electron density in the SNEP is not so different from that in the bulk compared with the case of the defects, resulting in the SNEPs and the bulk having almost the same positron lifetime as each other.

In this paper, we overcome the difficulties by measuring the positron annihilation time evolution of the momentum

distribution of electron-positron pairs by using the annihilation age-momentum correlation (AMOC) technique. Just after thermalization of the incident positrons, they are not yet trapped at the SNEPs, and thus they annihilate with the electrons of the host elements. During their diffusion, some of them get trapped at the SNEPs and annihilate with the electrons of the SNEPs. The AMOC method can sensitively pursue the time evolution of the momentum distributions in the high-momentum region which are specific to the chemical environment of the annihilation sites. Thus it gives information about the kinetics and the rate of positron trapping at the SNEPs, proportional to the number density, and also about the associated chemical element composition in the SNEPs.¹⁵

II. EXPERIMENT

Figure 1 shows a schematic diagram of the AMOC system. Time resolution of the conventional type of AMOC system which detects three γ rays in coincidence^{16,17} (one nuclear γ ray of 1.275 MeV used for the time of positron creation, and two annihilation γ rays of 511 keV, one used for the time of positron destruction and the other for measuring the momentum distribution) is typically 250–300 ps in full width at half maximum (FWHM). This is not enough for the present purpose because we have to analyze the elapsed time change within a time interval of a few hundred picoseconds. Here, to achieve a good time resolution ~ 170 ps in FWHM, we employed a digital oscilloscope. Wave shapes from two scintillation detectors and a high-purity Ge detector (HPGe) are directly recorded in the digital oscilloscope. They are analyzed offline for each annihilating event; the former is used to obtain positron age and the latter to obtain the momentum of electron-positron pairs. The method of analysis for positron age is the same as previously reported in Ref. 18. In order to reduce the source component, a $^{22}\text{NaCl}$ positron source of about 2 MBq was deposited directly on one of the samples and sandwiched with the other. The measurements were performed at room temperature.

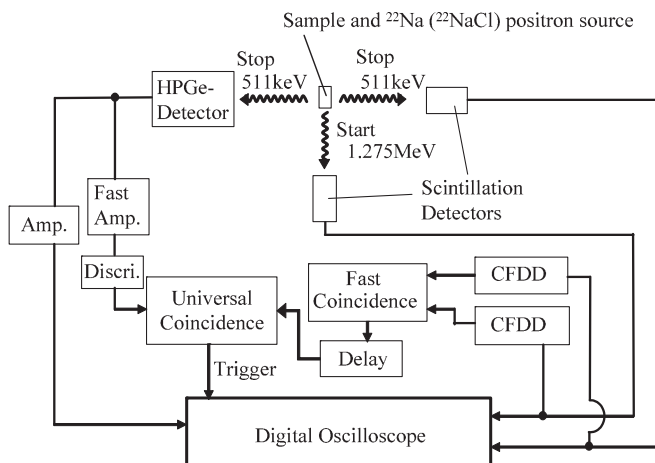


FIG. 1. Schematic diagram of our AMOC system using a digital oscilloscope. CFDD (constant fraction differential discriminator), HPGe (high-purity Ge detector), Amp (amplifier), and Discri (discriminator).

The material system employed in this study is Cu ultrafine particles embedded in Fe for the following reasons.¹⁹ (1) The embedded pure Cu particles of bcc structure coherent with the Fe matrix in the range between subnanometers and a few nanometers in diameter are easily obtained in Fe-Cu dilute alloys, and the size of the Cu particle can be well controlled by thermal aging. (2) Positron confinement in the Cu particles in Fe has been established.⁶ We prepared the Cu nanoparticle samples from a polycrystalline Fe–0.88 at.% Cu alloy by thermal aging. They were heated to 825°C and kept for 4 h, followed by quenching into ice water. The Cu atoms were isolated in a supersaturated solid solution in the as-quenched state. Then, the samples were thermally aged at 550°C for 0.1, 0.2, and 2.0 h after quenching; the Cu atoms are aggregated to form ultrafine particles in the range from subnanometers to a few nanometers in diameter.

III. RESULTS AND DISCUSSION

Figure 2 shows the annihilation time evolution of the high-momentum annihilation fraction $W(t)$ for the aged alloy samples, together with those for the pure Fe and Cu for reference. $W(t)$ is defined as

$$W(t) = \frac{\int_{p_1}^{p_2} N(p,t) dp}{\int N(p,t) dp} = \frac{\int_{p_1}^{p_2} N(p,t) dp}{L(t)}, \quad (1)$$

where $N(p,t)$ and $L(t)$ represent the AMOC spectrum and the lifetime spectrum, respectively. We adopted $p_1 = 10 \times 10^{-3} m_0 c$ and $p_2 = 22 \times 10^{-3} m_0 c$, where p is the longitudinal component of the electron-positron momentum along the γ -ray emission, m_0 is the electron (positron) rest mass, and c is the speed of light. $W(t)$ sensitively distinguishes the Cu electron momentum component from that of Fe because the above region well reflects the characteristic momentum distribution of $3d$ electrons ($3d^{10}$ for Cu and $3d^6$ for Fe).²⁰ $W(t)$ for the pure Cu [$W_{\text{Cu}}(t)$] can be easily distinguished

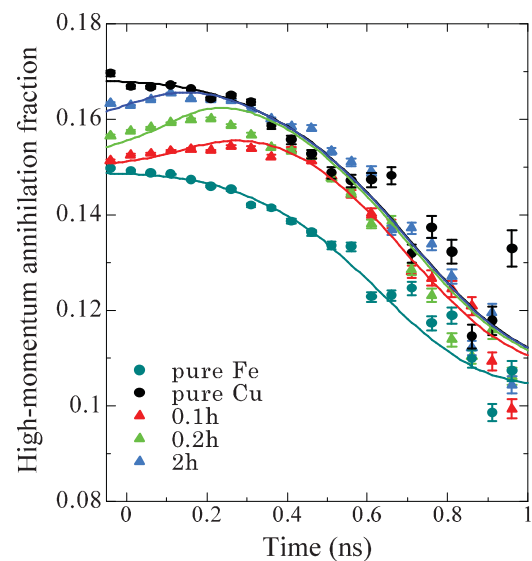


FIG. 2. (Color online) Positron annihilation time evolution of high-momentum annihilation fraction $W(t)$ for the Fe–0.88 at.% Cu alloy aged at 550 °C for 0.1, 0.2, and 2 h, together with those for pure Fe and Cu.

from that for the pure Fe [$W_{\text{Fe}}(t)$] in the time range shorter than ~ 1 ns. It is noteworthy that the $W_{\text{Cu}}(t)$ and $W_{\text{Fe}}(t)$ themselves should be independent of time in principle; however, in the experiments they decrease with time. This is because the long-lifetime components of the positron source with small W values become dominant with increasing time. Thus, this change has no physical meaning in the sample, and only the difference between the $W_{\text{Fe}}(t)$ and $W_{\text{Cu}}(t)$ is important. For the sample aged for 0.1 h the $W(t)$ at around time zero is almost equal to $W_{\text{Fe}}(t)$. In the initial stage up to 0.4 ns, the $W(t)$ increases gradually with time and becomes close to $W_{\text{Cu}}(t)$. The curve for the sample aged for 0.2 h shows a similar trend to that for 0.1 h, with a slightly larger value around time zero and becoming close to $W_{\text{Cu}}(t)$ in the initial stage. For the sample aged for 2 h, the $W(t)$ is almost the same as $W_{\text{Cu}}(t)$ in the whole time region except the very short time region around time zero.

This time evolution corresponds to the positron trapping kinetics mentioned above; just after thermalization (within a few picoseconds⁵) of the incident positrons, they are not yet trapped at the Cu particles, and then they dominantly annihilate with the electrons of Fe. During their diffusion, some of them get trapped at the Cu particles, annihilating with the Cu electrons. The specimen thermally aged for longer time shows that the positrons annihilate with the Cu electrons even in the earlier initial stage, which indicates that the positron trapping rate to the Cu particles become larger with thermal aging time. It should be also mentioned that all the $W(t)$ later than 0.5 ns become very close to $W_{\text{Cu}}(t)$ rather than $W_{\text{Fe}}(t)$, showing the saturation of positron trapping at the Cu particles and hence that positrons trapped at the Cu particles annihilate with the electrons of Cu, but not Fe, showing that the Cu particles consist of only Cu atoms (pure Cu particles).

We can estimate the positron trapping rate to the Cu particles directly from the experimental $W(t)$ by fitting with a curve based on a two-state trapping model^{5,7} as follows. First, the $W(t)$ for pure Fe (Cu) are successfully fitted with the following equation:

$$W_{\text{Fe(Cu)}}(t) = \left[(1 - I_{S1} - I_{S2}) W_{\text{Fe(Cu)}}^0 \lambda_{\text{Fe(Cu)}} e^{-\lambda_{\text{Fe(Cu)}} t} + I_{S1} W_{S1} \lambda_{S1} e^{-\lambda_{S1} t} + I_{S2} W_{S2} \lambda_{S2} e^{-\lambda_{S2} t} \right] / L_{\text{Fe(Cu)}}(t), \quad (2)$$

where $W_{\text{Fe(Cu)}}^0(t)$ and $\lambda_{\text{Fe(Cu)}}$ are the intrinsic high-momentum annihilation fractions other than the positron source and the annihilation rate for pure Fe (Cu), respectively. It should be noted that these intrinsic parameters $W_{\text{Fe(Cu)}}^0(t)$ and $\lambda_{\text{Fe(Cu)}}$ are time independent. W_{S1} and W_{S2} are the high-momentum annihilation fractions of the two source components. $I_{S1}, \lambda_{S1}, I_{S2}, \lambda_{S2}$ are the intensities and the annihilation rates for the two source components, respectively, being fixed parameters estimated from the lifetime spectrum

$$L_{\text{Fe(Cu)}}(t) = (1 - I_{S1} - I_{S2}) \lambda_{\text{Fe(Cu)}} e^{-\lambda_{\text{Fe(Cu)}} t} + I_{S1} \lambda_{S1} e^{-\lambda_{S1} t} + I_{S2} \lambda_{S2} e^{-\lambda_{S2} t} \quad (3)$$

obtained by integrating $N(p, t)$ over p . Second, the $W_{\text{FeCu}}(t)$ for the aged Fe-Cu samples are fitted as follows:

$$W_{\text{FeCu}}(t) = \left[(1 - I_{S1} - I_{S2}) \left(W_{\text{Fe}}^0 \lambda_{\text{Fe}} e^{-(\lambda_{\text{Fe}} + \kappa)t} + \frac{W_p \lambda_p \kappa}{\lambda_{\text{Fe}} + \kappa - \lambda_p} \{ e^{-\lambda_p t} - e^{-(\lambda_{\text{Fe}} + \kappa)t} \} \right) + I_{S1} W_{S1} \lambda_{S1} e^{-\lambda_{S1} t} + I_{S2} W_{S2} \lambda_{S2} e^{-\lambda_{S2} t} \right] / L_{\text{FeCu}}(t) \quad (4)$$

by using the parameters obtained above, where W_p and λ_p are the high-momentum annihilation fraction and the annihilation rate for the Cu particles, respectively,

$$L_{\text{FeCu}}(t) = (1 - I_{S1} - I_{S2}) \left(\lambda_{\text{Fe}} e^{-(\lambda_{\text{Fe}} + \kappa)t} + \frac{\lambda_p \kappa}{\lambda_{\text{Fe}} + \kappa - \lambda_p} \{ e^{-\lambda_p t} - e^{-(\lambda_{\text{Fe}} + \kappa)t} \} \right) + I_{S1} \lambda_{S1} e^{-\lambda_{S1} t} + I_{S2} \lambda_{S2} e^{-\lambda_{S2} t}, \quad (5)$$

and κ is the positron trapping rate which we have to determine. Here, we employed λ_p and W_p as the same values as λ_{Cu} and W_{Cu} , respectively, because the Cu particles are pure Cu as mentioned above.⁶ In the fitting process, the time resolution function and the background were corrected. The obtained positron trapping rate for the specimens aged for 0.1, 0.2, and 2.0 h are 4.1, 14, and 85 ns⁻¹, respectively, from the solid lines in Fig. 2.

The positron trapping rate κ is proportional to the number density of the Cu particles (C),²¹

$$\kappa = \mu C, \quad (6)$$

where μ represents the positron trapping coefficient. To estimate the number density we have to know the positron trapping coefficient. The positron trapping process is usually expressed by two regimes: positron diffusion limited and positron propagation ones.²¹ The positron trapping coefficient of the diffusion regime is given by

$$\mu_{\text{diff}} = 4\pi r D_+, \quad (7)$$

where D_+ is the positron diffusion coefficient, and r represents the effective radius for positron trapping which is assumed to be the average radius of the Cu particles. The positron trapping coefficient of the propagation regime is given by

$$\mu_{\text{prop}} = \sigma \nu_+, \quad (8)$$

where σ and ν_+ represent the positron capture cross section of the Cu particle and the positron thermal velocity, respectively. Here, we assumed that the overall positron trapping coefficient is given by following expression:^{22,23}

$$\frac{1}{\mu} = \frac{1}{\mu_{\text{diff}}} + \frac{1}{\mu_{\text{prop}}}. \quad (9)$$

We independently estimated the positron diffusion coefficients for Fe-Cu alloys with various Cu contents (0 to 0.88 at.%) from an experiment with an energy-variable positron beam²⁴ using the as-quenched alloys in which the Cu solute atoms were isolated in a supersaturated solid solution

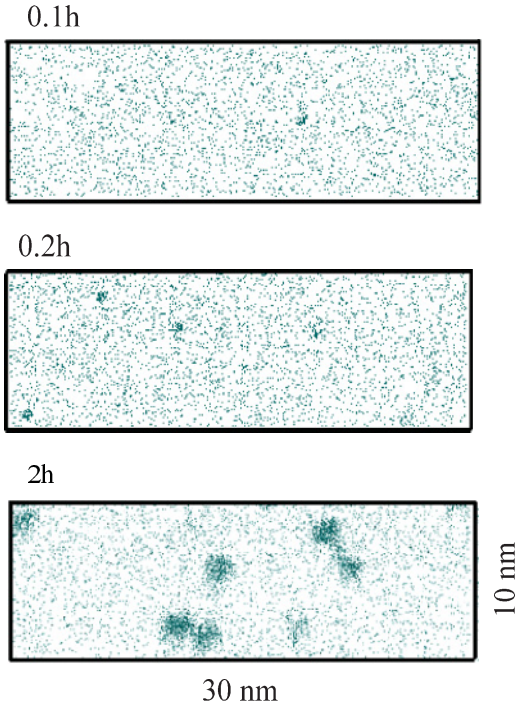


FIG. 3. (Color online) 3D atom maps of Cu atoms in the Fe-0.88 at.% Cu alloy samples aged for 0.1, 0.2, and 2 h by 3D-AP.

without forming Cu particles.⁶ At room temperature, the diffusion coefficients were about $2.0 \text{ cm}^2/\text{s}$ for all the alloys, almost independent of the Cu content, and thus we employed this value as D_+ . As for r , we obtained the radius of the Cu particles from 3D-AP observation. (3D-AP is a method for elemental mapping of metallic materials in three-dimensional real space with atomic-scale resolution.)^{2,3} Figure 3 shows examples of the 3D atom maps of Cu atoms for the thermally aged specimens. The obtained average radii are listed in Table I. We employed the effective mass of the positron ($m^* = 1.45m_0$) in Ref. 25 to obtain the ν_+ , and the cross section is assumed to be given by $\sigma = \pi r^2$.

Using these values, we estimated the number density of the Cu particles based on the results of AMOC as shown in Table I. As references, the number densities estimated by 3D-AP are also listed. The number densities from AMOC for the samples aged for 0.2 and 2 h agree well with those from 3D-AP. This clearly shows that the present method is justified to give the number density of the SNEPs. For the sample aged for 0.1 h, however, the number density estimated by 3D-AP is much

TABLE I. Average radii of the Cu embedded particles from 3D-AP and their number densities from AMOC and 3D-AP experiments.

Aging time (hour)	Radius (nm)	Number density ($\times 10^{17} \text{ cm}^{-3}$)	
		3D-AP	AMOC
0.1	0.45	0.15	0.71
0.2	0.55	1.2	1.6
2	1.25	1.9	2.1

lower than that by AMOC. This might be due to counting loss of the Cu subnanoparticles by 3D-AP, because it is difficult even for 3D-AP to detect such very small particles due to the ion detection efficiency of about 50% and the limit of the spatial resolution, as is seen from the atom map shown in Fig. 3. This suggests that the presented method is very useful for the SNEPs that other techniques cannot detect.

IV. SUMMARY

We demonstrated a method for the annihilation time evolution of the electron-positron momentum distribution to obtain the positron trapping rate and the chemical information about embedded subnano- and nanoparticles of Cu in Fe, using positron annihilation AMOC technique employing a digital oscilloscope with high time resolution. Unlike the case of open-volume trapping of positrons into vacancy-type defects, it is impossible to obtain the positron affinity trapping rate of SNEPs which are free from open-volume defects by conventional positron lifetime techniques. Furthermore, by analyzing the resultant trapping rate of Cu particles we successfully obtain the number densities of the Cu particles, even for the subnano Cu particles which are difficult to estimate by other experimental methods.

ACKNOWLEDGMENTS

This work is partly supported by Grants-in-Aid for Scientific Research of the Ministry of Education, Science and Culture (No. 17002009, No. 15106015, and No. 18686077), by the Toray Science Foundation, and by the Radioactive Waste Managing Funding and Research Center. One of the authors (Z.T.) is supported by the National Natural Science Foundation of China (NSFC).

¹D. B. Williams and C. Barry Carter, *Transmission Electron Microscopy: A Textbook for Materials Science*, 2nd ed. (Springer-Verlag, New York, 2009).

²T. F. Kelly and M. K. Miller, *Rev. Sci. Instrum.* **78**, 031101 (2007).

³M. K. Miller, *Atom Probe Tomography* (Kluwer Academic/Plenum Publishers, New York, 2000).

⁴A. Ulbricht, F. Bergner, J. Bohmert, M. Valo, M. H. Mathon, and A. Heinemann, *Philos. Mag.* **87**, 1855 (2007).

⁵*Positron Spectroscopy of Solids*, edited by A. Dupasquier and A. P. Mills Jr. (IOS Press, Amsterdam, 1995).

⁶Y. Nagai, M. Hasegawa, Z. Tang, A. Hempel, K. Yubuta, T. Shimamura, Y. Kawazoe, A. Kawai, and F. Kano, *Phys. Rev. B* **61**, 6574 (2000).

⁷M. J. Puska and R. M. Nieminen, *Rev. Mod. Phys.* **66**, 841 (1994).

⁸M. Hasegawa, Z. Tang, Y. Nagai, T. Chiba, E. Kuramoto, and M. Takenaka, *Philos. Mag.* **85**, 467 (2005).

⁹G. Dlubek, *Mater. Sci. Forum* **13-14**, 11 (1987).

- ¹⁰Y. Nagai, Z. Tang, M. Hasegawa, T. Kanai, and M. Saneyasu, *Phys. Rev. B* **63**, 134110 (2001).
- ¹¹Y. Nagai, T. Chiba, Z. Tang, T. Akahane, T. Kanai, M. Hasegawa, M. Takenaka, and E. Kuramoto, *Phys. Rev. Lett.* **87**, 176402 (2001).
- ¹²Y. Nagai, T. Toyama, Z. Tang, K. Inoue, T. Chiba, M. Hasegawa, S. Hirose, and T. Sato, *Phys. Rev. B* **79**, 201405(R) (2009).
- ¹³Z. Tang, T. Toyama, Y. Nagai, K. Inoue, Z. Q. Zhu, and M. Hasegawa, *J. Phys. Condens. Matter* **20**, 445203 (2008).
- ¹⁴T. Toyama, Z. Tang, K. Inoue, T. Chiba, T. Ohkubo, K. Hono, Y. Nagai, and M. Hasegawa (unpublished).
- ¹⁵The conventional CDB method [P. Asoka-Kumar, M. Alatalo, V. J. Ghosh, A. C. Kruseman, B. Nielsen, and K. G. Lynn, *Phys. Rev. Lett.* **77**, 2097 (1996)] may be expected to estimate the positron trapping rate to the SNEPs: From the annihilation fraction with the elements of the SNEP, the positron trapping fraction to the SNEP can be estimated. However, this is possible only when the chemical composition of the SNEP is known.
- ¹⁶N. Suzuki, Y. Nagai, and T. Hyodo, *Phys. Rev. B* **60**, R9893 (1999).
- ¹⁷N. Suzuki, Y. Nagai, Y. Itoh, A. Goto, Y. Yano, and T. Hyodo, *Phys. Rev. B* **63**, 180101(R) (2001).
- ¹⁸H. Saito and T. Hyodo, *Phys. Rev. Lett.* **90**, 193401 (2003).
- ¹⁹In the nuclear industry, ultrafine Cu rich subnanoprecipitates whose diameters are less than 2 nm are considered to be one of the origins of the embrittlement [W. J. Phythian and C. A. English, *J. Nucl. Mater.* **205**, 162 (1993)] in the end of life of old nuclear reactor pressure vessels. Therefore, it is of critical importance to elucidate the very initial stage of the Cu precipitation for the safe operation of nuclear power plants.
- ²⁰Z. Tang, M. Hasegawa, Y. Nagai, and M. Saito, *Phys. Rev. B* **65**, 195108 (2002).
- ²¹W. Brandt, *Appl. Phys.* **5**, 1 (1974).
- ²²M. Eldrup and K. O. Jensen, *Phys. Status Solidi A* **102**, 145 (1987).
- ²³R. Krause-Rehberg and H. S. Leipner, *Positron Annihilation in Semiconductors* (Springer-Verlag, Berlin, 1999).
- ²⁴E. Soininen, H. Huomo, P. A. Huttunen, J. Makinen, A. Vehanen, and P. Hautajarvi, *Phys. Rev. B* **41**, 6227 (1990).
- ²⁵G. Fletcher, J. L. Fry, and P. C. Pattnaik, *Phys. Rev. B* **27**, 3987 (1983).